Chemical Physics Letters 740 (2020) 137078

Contents lists available at ScienceDirect

Chemical Physics Letters

journal homepage: www.elsevier.com/locate/cplett

Research paper

SnO_2 interlayer effects on the inverted polymer solar cells

Yunus Özen[a,b], İdris Candan[c,*]

[a] Gazi University, Faculty of Science, Department of Physics, 06500 Ankara, Turkey
[b] Gazi University, Photonics Application and Research Center, Ankara, Turkey
[c] Kocaeli University, Department of Physics, 41001 Izmit, Kocaeli, Turkey

HIGHLIGHTS

- The thin film layers of SnO_2 and TiO_2 were deposited by sputtering technique.
- The SnO_2 interlayer was successfully inserted in between FTO and TiO_2/P3HT:PCBM layers.
- The relative increase in PCE was calculated as 31.7% by adding SnO_2 interlayer.

ARTICLE INFO

Keywords:
Inverted Polymer Solar Cells (IPSC)
Power Conversion Efficiency (PCE)
SnO_2 and TiO_2

ABSTRACT

By inserting a tin oxide (SnO_2) thin film layer in between Fluorine-doped Tin Oxide (FTO) and titanium dioxide (TiO_2) electron-selective layers, the performance of P3HT: PCBM based bulk-heterojunction type inverted polymer solar cells is considerably enhanced. A device with adding SnO_2 layer showed a significant increase in PCE of 2.87% with an improved short-circuit current from 6.8 mA/cm^2 to 10.40 mA/cm^2, compared to a reference device without SnO_2 layer (2.18%). The relative increase in PCE value was 31.7%. Such enhancement is assigned to the excellent optical transparency and high electrical conductivity of the wide-band gap of SnO_2 thin film layer.

1. Introduction

Polymer-fullerene based bulk heterojunction (BHJ) materials have been widely used in the field of photovoltaic (PV) solar cell applications over the past decades due to the simple synthesis materials, cost-effective coating process and energy sources [1-3]. However, to make polymer solar cells an alternative for traditional PV technology, the efficiency values of polymer solar cell need further improvement. In contrast to traditional PV cells, a strongly bound positive and negative charge carriers (excitons) are created in the bulk heterojunction (BHJ) and only diffuse throughout their lifetime of about 5–10 nm in organic materials [4–6]. Additionally, the exciton decomposition and charge recombination affect in cutting down numbers of free carriers traveling to opposite electrodes [7]. The PCE of polymer solar cells decreases due to the degeneration of charge collection property and transport ability of ITO layer [8,9]. To overcome these issues, a buffer layer of metal oxide such as TiO_2, ZnO or SnO_2 is inserted in between FTO or ITO electrode and polymer photoactive layers to collect generated charge carriers before recombination. This configuration of PV device is known as inverted polymer solar cell (IPSC) [10,11]. Moreover, in order to enhance the performance of solar cell, the longer exciton diffusion length is needed [12,13].

It is common to use different interlayers to increase the PCE value of solar cells and improve the transport of electrons and holes. Bakr et al. inserted SnO_2 interlayer in between FTO and TiO_2 layers in for dye-sensitized solar cells (DSSCs). They improved the cell efficiency from 5.1 to 8.0% [14]. Lee et al. used polyethylenimine ethoxylated (PEIE) interlayer and improved the PCE value of IPSC from 1.2 to 2.0% [15]. Molybdenum oxide (MoO_3) interlayer was used to study interlayer effects on different type organic photovoltaic cells by Kim et al. The MoO_3 interlayer improved the PCE value from 2.85 to 3.31% [16]. Rao et al. enhanced the perovskite solar cells (PSCs) by inserting a SnO_2 nanocolloid interlayer in between FTO and $TiCl_4$ layers. The PCE value of PSCs dramatically increased from 6.52 to 14.69% after inserting the SnO_2 nanocolloid interlayer [17].

Thin films of TiO_2 and SnO_2 are widely studied in the field of polymer based PV due to their suitable structural, electrical and optical properties [18,19]. These materials can be employed as a protective and anti-reflective coating on FTO/ITO because of their seamless optical transmittance, good insulating abilities and effectiveness in

* Corresponding author.
E-mail address: idris.candan@kocaeli.edu.tr (İ. Candan).

https://doi.org/10.1016/j.cplett.2019.137078
Received 22 October 2019; Received in revised form 21 December 2019; Accepted 30 December 2019
Available online 31 December 2019
0009-2614/ © 2019 Elsevier B.V. All rights reserved.

reducing the recombination [20-22]. Among these materials, SnO_2 thin film as a buffer layer for organic optoelectronic devices has recently received special interest for its excellent properties such as high optical transparency, desirable band alignment and high electron mobility [23-25]. The electrical conductivities of SnO_2 thin films change in between 10^2 and 10^3 $(\Omega\ cm)^{-1}$, while the electrical conductivities of TiO_2 thin films change in between 0.1 and 10 $(\Omega\ cm)^{-1}$ [26,27] depending on growth conditions. Moreover, the SnO_2 thin film has a band gap value of 3.6 eV while the FTO layer has band gap value of 3.8 eV and TiO_2 thin film has the band gap value of 3.2 eV. Therefore, inserting the SnO_2 interlayer in between FTO and TiO_2 layers can make suitable material for favorable band alignment and transporting the electrons between these layers [28–30].

The main objective of this work was to enhance metal oxide layer of TiO_2 and collect charge carriers before recombination by deposition of 10 nm SnO_2 thin film in between FTO and TiO_2 layer. The SnO_2 layer was placed in between the glass/FTO and TiO_2/P3HT:PCBM layers to use as an electron transport layer (ETL) and hole blocking layer. The presence of this layer inside the structure significantly reduces the reverse saturation current in between the glass/FTO and TiO_2/P3HT:PCBM layers. The performances of IPSC have been compared with and without SnO_2 layer. The values of PCE and short circuit current have been successfully improved by placing the SnO_2 thin film layer.

2. Experimental method

In order to study the effects of SnO_2 layer inside polymer based IPSC, two different (with and without SnO_2 layer) devices were fabricated onto high quality FTO coated glass substrates as illustrated in Fig. 1. Two steps cleaning process was applied to commercially purchased FTO coated glass substrate with optical transmittance of 85% by using the ultrasonic bath before thin film deposition steps to eliminate the unwanted organic and inorganic contaminations. 10 nm of SnO_2 layer was deposited on cleaned FTO surfaces by Nanovak NVTS500 co-sputtering system. To compare effects of SnO_2 layer, 75 nm TiO_2 layer was fabricated on top of Glass/FTO and Glass/FTO/SnO_2 substrates by using sputtering system under the 10^{-6} Torr vacuum.

A solution of blended P3HT:PCBM was spin coated onto Glass/FTO/SnO_2/TiO_2 and Glass/FTO/TiO_2 substrates with 600 rpm for 20 s and 1100 rpm for 9 s at room temperature. Then, heat treatment was applied to samples at 150 °C for 5 min by a hot plate. The anode buffer layer (ABL) of molybdenum trioxide (MoO_3) with 10 nm and the top electrode of the silver (Ag) with 100 nm were thermaly deposited on top of Glass/FTO/SnO_2/TiO_2/P3HT:PCBM and Glass/FTO/TiO_2/P3HT:PCBM samples, respectively. Fig. 1(e) shows the picture of IPSC.

Transmittance spectra of glass, Glass/TiO_2 and Glass/SnO_2/TiO_2 were executed in between 300 and 1100 nm wavelength range by Perkin Elmer Lambda-2S UV–Vis–NIR spectrometer system. AFM images of SnO_2, TiO_2 and P3HT:PCBM were obtained by NanoMagnetics Instruments. The current density-voltage (J-V) measurements were studied by a Keithley 4200 Sourcemeter and Newport Oriel-Sol1A solar simulator was performed to generate AM 1.5G illumination.

3. Results and discussions

Fig. 2 shows the UV-Vis-NIR transmittance spectra measured for glass, Glass/TiO_2 and Glass/SnO_2/TiO_2 from 300 to 1100 nm. As seen from figure, the transmittance spectra of Glass/TiO_2 and Glass/SnO_2/TiO_2 are similar and the maximum transmission is around 78%, which is enough to create the electron-hole pairs in the photoactive layer. Furthermore, the transparency of the Glass/SnO_2/TiO_2 structure is the same as the Glass/TiO_2 structure. Although no loss from SnO_2 thin film layer occurs, the transparency remains the same despite an increase in total thickness. This shows that the SnO_2 thin film structure is highly

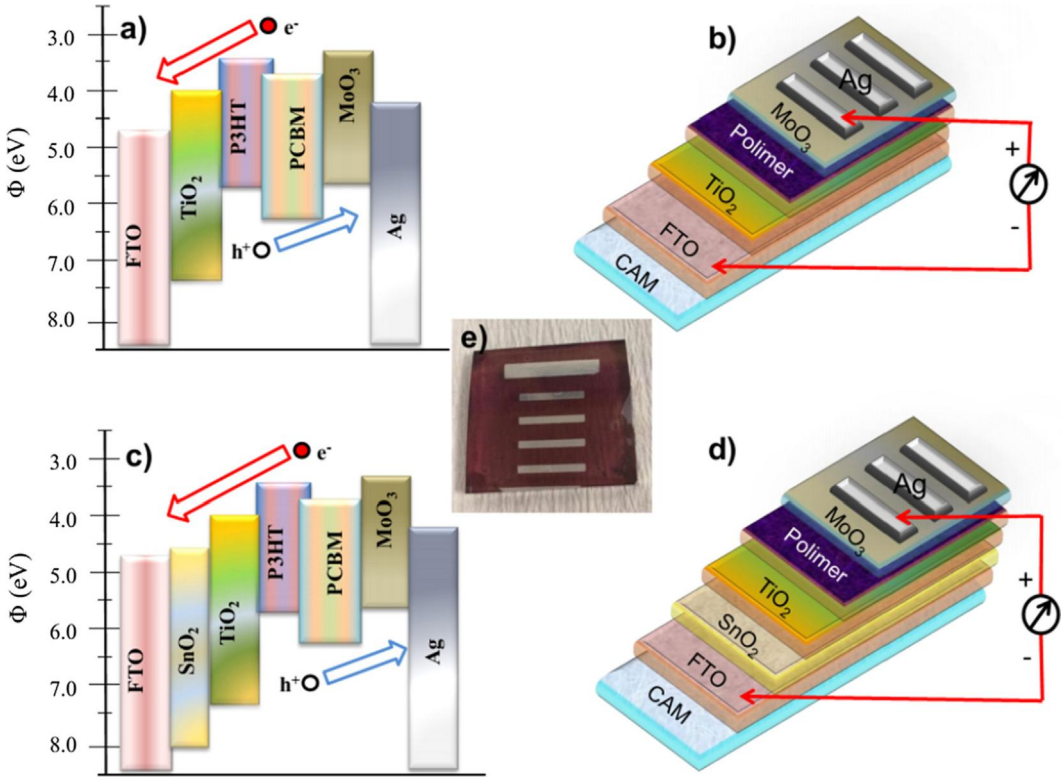


Fig. 1. Schematic representations of (a) band position diagram and (b) fabricated IPSC device without SnO_2 layer containing Glass/FTO/TiO_2/P3HT:PCBM/MoO_3/Ag layers, (c) band position diagram and (d) fabricated IPSC device with SnO_2 layer containing Glass/FTO/SnO_2/TiO_2/P3HT:PCBM/MoO_3/Ag layers. (e) The picture of completed IPSC device.

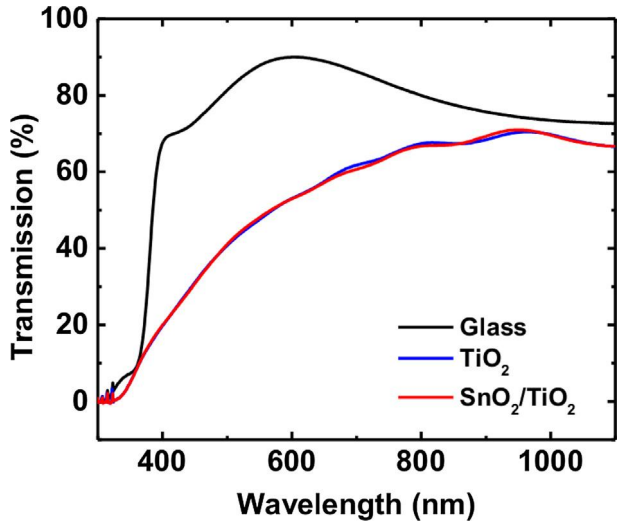


Fig. 2. (a) Transmittance (T) spectra of glass, Glass/TiO_2 and Glass/SnO_2/TiO_2 samples.

transparent and SnO_2 layer minimizes the loss of photons before reaching the photoactive polymer layer. Furthermore, the relatively high transparency of the thin film indicates that it has low surface roughness and good homogeneity.

The surface morphology of the fabricated IPCS structures of Glass/FTO/SnO_2, Glass/FTO/SnO_2/TiO_2 and Glass/FTO/SnO2/TiO2/P3HT:PCBM was carried out by a high performance AFM at room temperature. Fig. 3 presents the two-dimensional (2D) AFM topographic images captured from the scanning area surface of 20x20 μm^2 of SnO_2, TiO_2 and P3HT:PCBM polymer layers. The root-mean-square (RMS) roughness values measured from the topography images were 2.24 nm, 4.20 nm and 2.41 nm for SnO_2 (Fig. 3(a)), TiO_2 (Fig. 3(b)) and P3HT: PCBM (Fig. 3(c)) films, respectively. The very different morphology of these three thin films suggests that the interactions between the molecules of each thin film layer may be differently effect the PCE value (farther investigation required). Fig. 3(a) and (b) demonstrate that SnO_2 and TiO_2 thin films have crystalline surface morphology. However, the surface of the sample has turned into nodule-like structure and become smoother with coating polymer layer as given in Fig. 3(c). The noodle-like structure is generally associated with the crystallinity of the layer and thus increases the PCE. This points out that the morphology and PCE in the new polymer systems have a significantly different correlation from conventional solar cell structures [3].

To study the effects of SnO_2 thin film layer on IPSC, the current density as a function of reverse and forward voltage measurements of Glass/FTO/TiO_2/Polymer/MoO_3/Ag and Glass/FTO/SiO_2/TiO_2/Polymer/MoO_3/Ag samples were carried out under AM1.5G illumination. Fig. 4 shows current density-voltage (*J-V*) and semi-logarithmic current density-voltage (*Log (J)-V*) characteristics of IPSC for applied DC bias voltages at room temperature with and without SnO_2 thin film layer. The PCE and other device parameters were computed from *J-V* curves and the variation in the PCE, short-circuit current (J_{SC}), open-circuit voltage (V_{OC}) and fill factor (*FF*) are given in Table 1. The PCE values of IPSC with and without SnO_2 layer was calculated as 2.87 and 2.18%, respectively. The relative improvement of PCE with adding SnO_2 is 31.7%. The PCE improvement in the device is mainly due to the bigger J_{SC} (6.8 mA/cm^2 to 10.40 mA/cm^2) and the hybridization of SnO_2 and TiO_2 electron-selective layers. There are two basic mechanisms for the transfer of electrons from TiO_2 layer to SnO_2 layer. The first transfer mechanism occurs due to the higher work function of SnO_2 and the higher affinity of TiO_2. The second transfer mechanism takes place because the paired layers with different conductive band edges provide excellent charge separation as a result of rapid electron transfer from TiO_2 layer to SnO_2 layer. Hence, the SnO_2/TiO_2 double-layered film is irradiated by photons, a greater number of electrons transfer from TiO_2 thin film layer to SnO_2 thin film layer [31]. Additionally, charge recombination between an injected electron and a polymer photoactive layer takes place on much longer time scales for SnO_2/TiO_2 double-layered material than for TiO_2 layer alone [32]. The hybridization of layers collected the excitons before recombination and that improved the short-circuit current. The relative increase in J_{SC} value was computed as 53% for the device with SnO_2 interlayer. On the contrary, the value of V_{OC} and *FF* decreased with the addition of SnO_2 as shown in the Table 1. The value of V_{OC} decreased from 0.85 to 0.78 V, while *FF* decreased from 38 to 35%. The decrease in V_{OC} and FF for the cell with SnO_2 thin film interlayer might cause by tunneling effect due to the thickness of the energy barrier. The SnO_2 thin film interlayer should be a certain thickness because the electron tunneling depends on the thickness of the energy barrier [30,33-35]. If the certain thickness value of the barrier is exceeded, the created electron will be transported through the SnO_2 interlayer by tunneling effect, and therefore the V_{OC} and FF values of the solar cell will decrease. On the other hand, the values of PCE and short-circuit current (J_{SC}) of cell with SnO_2 interlayer increased due to the SnO_2 layer absorbed more light but the PCE value remained low due to the decrease in Voc value caused by electron tunneling. If the SnO_2 layer thickness is kept less than the certain thickness value, the electric shorting and pinholes might be developed at the SnO_2/TiO_2 junction and the V_{OC} and FF will inevitably be decreased [36]. Further investigation is under way to provide more information about the optimum thickness of SnO_2 thin film interlayer.

4. Conclusions

In summary, P3HT:PCBM based IPSC with inserted-SnO_2 layers were fabricated and examined. Incorporation of SnO_2 layer into IPSC

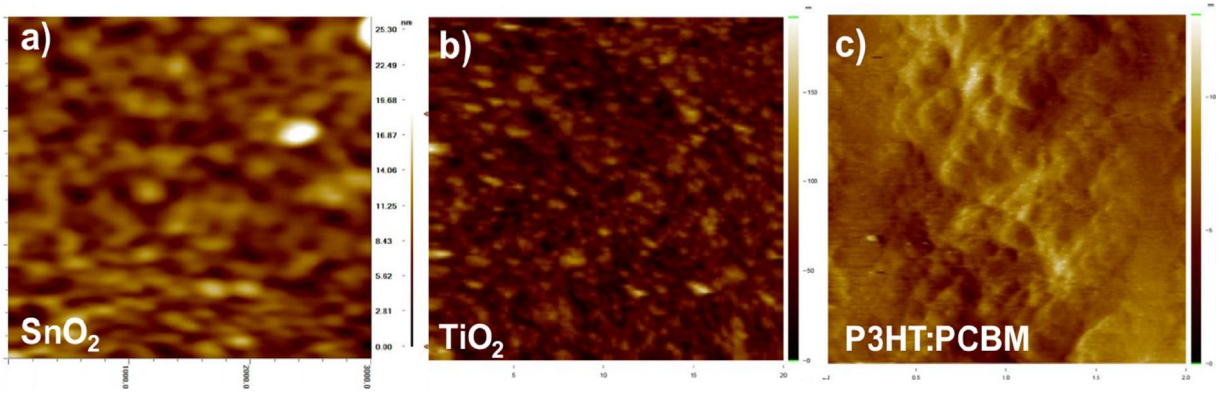


Fig. 3. AFM images of the 2D configuration of (a) SnO_2, (b) TiO_2, and (c) P3HT:PCBM thin films.

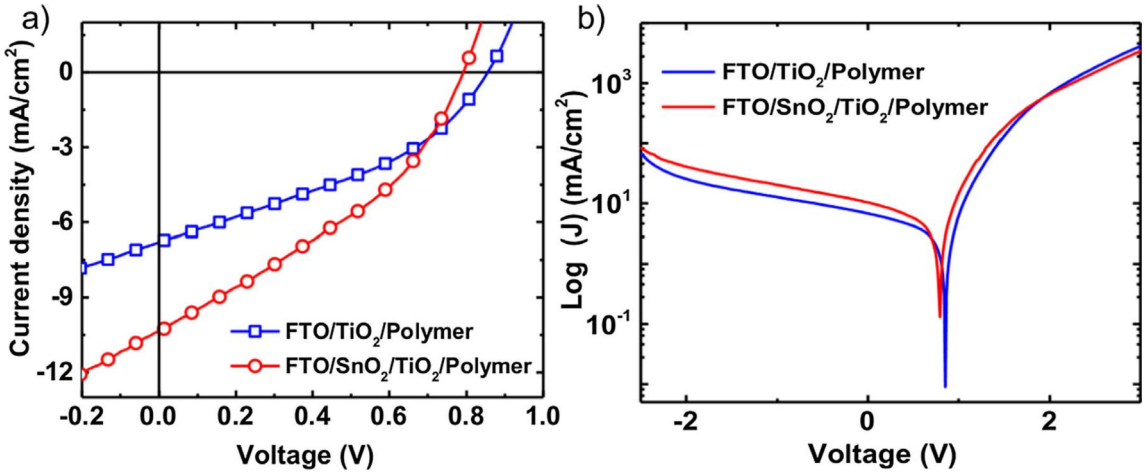


Fig. 4. (a) The current density (J)–voltage (V) and (b) semi-logarithmic current density-voltage characteristics of the IPSC devices without and with SnO_2 layer under illumination of AM 1.5G.

Table 1
Summary of the photovoltaic performance parameters of the IPSC with and without SnO_2 layer.

Sample	J_{SC}(mA/cm^2)	V_{OC}(V)	FF(%)	η(%)
FTO/TiO_2/Polymer	6.8	0.85	38	2.18
FTO/SnO_2/TiO_2/Polymer	10.4	0.78	35	2.87

structure in between FTO and TiO_2 electron-selective layers improved the device performance. It was deduced that additional layer of SnO_2 created hybridization with TiO_2 and enhanced the electron-selective layer. The calculated PV parameters from *J-V* measurements showed that hybridization of two layers improved the device efficiency by collecting free charge carriers in the polymer photoactive layer which increased J_{SC}.

Author contributions

İ.C & Y.Ö conceived the study, synthesized materials, conducted experiments, and performed data analysis. The manuscript prepared by İ.C. and guided by all authors. Material processing conducted by İ.C. & Y.Ö. AFM measurements were performed by İ.C. Transmission and J-V measurements were performed by Y.Ö. Data analysis of the AFM, Transmission and J-V measurements was perfomed by İ.C.

CRediT authorship contribution statement

Yunus Özen: Methodology, Data curation, Visualization, Investigation, Software, Validation, Writing - review & editing. **İdris Candan:** Conceptualization, Methodology, Visualization, Writing - original draft, Software, Supervision, Writing - review & editing.

Declaration of Competing Interest

The authors declare that they have no known competing financial interests or personal relationships that could have appeared to influence the work reported in this paper.

Acknowledgments

This work was partially supported by The Presidency of Strategy and Budget, Turkey under the project number of 2016K121220.

Appendix A. Supplementary material

Supplementary data to this article can be found online at https://doi.org/10.1016/j.cplett.2019.137078.

References

[1] R. Steim, S.A. Choulis, P. Schilinsky, C.J. Brabec, Interface modification for highly efficient organic photovoltaics, Appl. Phys. Lett. 92 (2008) 2006–2009, https://doi.org/10.1063/1.2885724.
[2] S.S. Van Bavel, M. Bärenklau, G. De With, H. Hoppe, J. Loos, P3HT/PCBM bulk heterojunction solar cells: Impact of blend composition and 3D morphology on device performance, Adv. Funct. Mater. 20 (2010) 1458–1463, https://doi.org/10.1002/adfm.200902247.
[3] H.-Y. Chen, J. Hou, S. Zhang, Y. Liang, G. Yang, Y. Yang, L. Yu, Y. Wu, G. Li, Polymer solar cells with enhanced open-circuit voltage and efficiency, Nat. Photon. 3 (2009) 649–653, https://doi.org/10.1038/nphoton.2009.192.
[4] W.J.E. Beek, L.H. Slooff, M.M. Wienk, J.M. Kroon, R.A.J. Janssen, Hybrid solar cells using a zinc oxide precursor and a conjugated polymer, Adv. Funct. Mater. 15 (2005) 1703–1707, https://doi.org/10.1002/adfm.200500201.
[5] J.J.M. Halls, K. Pichler, R.H. Friend, S.C. Moratti, A.B. Holmes, Exciton diffusion and dissociation in a poly(p-phenylenevinylene)/C60 heterojunction photovoltaic cell, Appl. Phys. Lett. 68 (1996) 3120, https://doi.org/10.1063/1.115797.
[6] E. Bundgaard, F. Krebs, Low band gap polymers for organic photovoltaics, Sol. Energy Mater. Sol. Cells. 91 (2007) 954–985, https://doi.org/10.1016/j.solmat.2007.01.015.
[7] D.C. Nguyen, N.D. Nguyen, D.L. Nguyen, H.-K. Kim, P.H.N. Nguyen, Characterization of performance parameters of organic solar cells with a buffer ZnO layer, Adv. Nat. Sci. Nanosci. Nanotechnol. 10 (2019) 015005, https://doi.org/10.1088/2043-6254/aafda1.
[8] M. Jørgensen, K. Norrman, F.C. Krebs, Stability/degradation of polymer solar cells, Sol. Energy Mater. Sol. Cells. 92 (2008) 686–714, https://doi.org/10.1016/j.solmat.2008.01.005.
[9] F.C. Krebs, K. Norrman, Analysis of the failure mechanism for a stable organic photovoltaic during 10 000 h of testing, Prog. Photovoltaics Res. Appl. 15 (2007) 697–712, https://doi.org/10.1002/pip.794.
[10] Y. Şahin, S. Alem, R. de Bettignies, J.-M. Nunzi, Development of air stable polymer solar cells using an inverted gold on top anode structure, Thin Solid Films. 476 (2005) 340–343, https://doi.org/10.1016/J.TSF.2004.10.018.
[11] M. Glatthaar, M. Niggemann, B. Zimmermann, P. Lewer, M. Riede, A. Hinsch, J. Luther, Organic solar cells using inverted layer sequence, Thin Solid Films. 491 (2005) 298–300, https://doi.org/10.1016/J.TSF.2005.06.006.
[12] S. Kundu, A. Patra, Nanoscale Strategies for Light Harvesting, Chem. Rev. 117 (2017) 712–757, https://doi.org/10.1021/acs.chemrev.6b00036.
[13] B. Guzelturk, H.V. Demir, Organic−inorganic composites of semiconductor nanocrystals for efficient excitonics hybrids of conjugated polymers− colloidal nanocrystals are needed to boost the excitonic interac-tions without suffering from phase segregation, J. Phys. Chem. Lett. 6 (2015) 2206–2215, https://doi.org/10.1021/acs.jpclett.5b00415.
[14] Z.H. Bakr, Q. Wali, J. Ismail, N.K. Elumalai, A. Uddin, R. Jose, Synergistic combination of electronic and electrical properties of SnO2 and TiO2 in a single SnO2-TiO2 composite nanofiber for dye-sensitized solar cells, Electrochim. Acta. 263 (2018) 524–532, https://doi.org/10.1016/j.electacta.2018.01.074.
[15] D.J. Lee, D.K. Heo, C. Yun, Y.H. Kim, M.H. Kang, Solution-processed semi-transparent inverted organic solar cells from a transparent conductive polymer electrode, ECS J. Solid State Sci. Technol. 8 (2019) Q32–Q37, https://doi.org/10.1149/2.0231902jss.
[16] Do Young Kim, Jegadesan Subbiah, Galileo Sarasqueta, Franky So, Huanjun Ding, Irfan, Yongli Gao, The effect of molybdenum oxide interlayer on organic photovoltaic cells, Appl. Phys. Lett. 95 (9) (2009) 093304, https://doi.org/10.1063/1.3220064.
[17] H.-S. Rao, B.-X. Chen, W.-G. Li, Y.-F. Xu, H.-Y. Chen, D.-B. Kuang, C.-Y. Su, Improving the extraction of photogenerated electrons with SnO2 nanocolloids for

efficient planar perovskite solar cells, Adv. Funct. Mater. 25 (2015) 7200–7207, https://doi.org/10.1002/adfm.201501264.
[18] C. Martinet, V. Paillard, A. Gagnaire, J. Joseph, Deposition of SiO2 and TiO2 thin films by plasma enhanced chemical vapor deposition for antireflection coating, J. Non. Cryst. Solids. 216 (1997) 77–82, https://doi.org/10.1016/S0022-3093(97)00175-0.
[19] S. Trost, K. Zilberberg, A. Behrendt, T. Riedl, Room-temperature solution processed SnOxas an electron extraction layer for inverted organic solar cells with superior thermal stability, J. Mater. Chem. 22 (2012) 16224–16229, https://doi.org/10.1039/c2jm33445c.
[20] W.-P. Tai, Photoelectrochemical properties of SnO2/TiO2 coupled electrode sensitized by a mercurochrome dye, Mater. Lett. 51 (2001) 451–454, https://doi.org/10.1016/S0167-577X(01)00433-5.
[21] C. Wang, C. Shao, X. Zhang, Y. Liu, SnO2 nanostructures-TiO2 nanofibers heterostructures: controlled fabrication and high photocatalytic properties, Inorg. Chem. 48 (2009) 7261, https://doi.org/10.1021/ic9005983.
[22] S. Yu, W. Yang, L. Li, W. Zhang, Improved chemical stability of ITO transparent anodes with a SnO2 buffer layer for organic solar cells, Sol. Energy Mater. Sol. Cells. 144 (2016) 652–656, https://doi.org/10.1016/j.solmat.2015.10.005.
[23] J. Sun, A. Lu, L. Wang, Y. Hu, Q. Wan, High-mobility transparent thin-film transistors with an Sb-doped SnO2 nanocrystal channel fabricated at room temperature, Nanotechnology 20 (2009) 335204, , https://doi.org/10.1088/0957-4484/20/33/335204.
[24] F. Yang, S.R. Forrest, Organic solar cells using transparent SnO2–F anodes, Adv. Mater. 18 (2006) 2018–2022, https://doi.org/10.1002/adma.200600797.
[25] M.F.M. Noh, M.F. Soh, C.H. Teh, E.L. Lim, C.C. Yap, M.A. Ibrahim, N.A. Ludin, M.A.M. Teridi, Effect of temperature on the properties of SnO 2 layer fabricated via AACVD and its application in photoelectrochemical cells and organic photovoltaic devices, Sol. Energy. 158 (2017) 474–482, https://doi.org/10.1016/j.solener.2017.09.048.
[26] J. Nowotny, M. Radecka, M. Rekas, Semiconducting properties of undoped TiO2, J. Phys. Chem. Solids. 58 (1997) 927–937, https://doi.org/10.1016/S0022-3697(96)00204-1.
[27] A. Yildiz, S.B. Lisesivdin, M. Kasap, D. Mardare, Electrical properties of TiO2 thin films, J. Non. Cryst. Solids. 354 (2008) 4944–4947, https://doi.org/10.1016/j.jnoncrysol.2008.07.009.
[28] N. Chiodini, A. Paleari, D. Dimartino, G. Spinolo, SnO2 nanocrystals in SiO2: A wide-band-gap quantum-dot system, Appl. Phys. Lett. 81 (2002) 1702–1704, https://doi.org/10.1063/1.1503154.
[29] S.K. Sahoo, S. Pal, P. Sarkar, C. Majumder, Size-dependent electronic structure of rutile TiO2 quantum dots, Chem. Phys. Lett. 516 (2011) 68–71, https://doi.org/10.1016/j.cplett.2011.09.047.
[30] X. Li, K. Shen, Q. Li, Y. Deng, P. Zhu, D. Wang, Roll-over behavior in current-voltage curve introduced by an energy barrier at the front contact in thin film CdTe solar cell, Sol. Energy. 165 (2018) 27–34, https://doi.org/10.1016/j.solener.2018.02.075.
[31] H.-C. Lee, W.-S. Hwang, Substrate effects on the oxygen gas sensing properties of SnO2/TiO2 thin films, Appl. Surf. Sci. 253 (2006) 1889–1897, https://doi.org/10.1016/j.apsusc.2006.03.036.
[32] E.M. James, T.J. Barr, G.J. Meyer, Evidence for an electronic state at the interface between the SnO2 core and the TiO2 shell in mesoporous SnO2 /TiO2 thin films, ACS Appl. Energy Mater. 1 (2018) 859–867, https://doi.org/10.1021/acsaem.7b00274.
[33] J. Fritsche, D. Kraft, A. Thißen, T. Mayer, A. Klein, W. Jaegermann, Band energy diagram of CdTe thin film solar cells, Thin Solid Films. 403–404 (2002) 252–257, https://doi.org/10.1016/S0040-6090(01)01528-0.
[34] N. Abdollahi, N.E. Gorji, Modeling the charge density profile in thin film devices using SIMS profiling data, Superlatt. Microstruct. 100 (2016) 9–13, https://doi.org/10.1016/j.spmi.2016.08.024.
[35] A. Niemegeers, M. Burgelman, Effects of the Au/CdTe back contact on IV and CV characteristics of Au/CdTe/CdS/TCO solar cells, J. Appl. Phys. 81 (1997) 2881–2886, https://doi.org/10.1063/1.363946.
[36] R. Yang, D. Wang, L. Wan, D. Wang, High-efficiency CdTe thin-film solar cell with a mono-grained CdS window layer, RSC Adv. 4 (2014) 22162–22171, https://doi.org/10.1039/C4RA01394H.